Alternative pathways of dewetting for a thin liquid two-layer film

Andrey Pototsky, Michael Bestehorn, and Domnic Merkt
Lehrstuhl für Theoretische Physik II, Brandenburgische Technische Universität Cottbus,
Erich-Weinert-Straße 1, D-03046 Cottbus, Germany

Uwe Thiele
Max-Planck-Institut für Physik komplexer Systeme, Nöthnitzer Straße 38, D-01187 Dresden, Germany

We consider two stacked ultrathin layers of different liquids on a solid substrate. Using long-wave theory, we derive coupled evolution equations for the free liquid-liquid and liquid-gas interfaces. Depending on the long-range van der Waals forces and the ratio of the layer thicknesses, the system follows different pathways of dewetting. The instability may be driven by varicose or zigzag modes and leads to film rupture either at the liquid-gas interface or at the substrate. We predict that the faster layer drives the evolution and may accelerate the rupture of the slower layer by orders of magnitude, thereby promoting the rupture of rather thick films.

Instability phenomena in ultrathin soft matter films with thicknesses below 100 nm became relevant mainly because they obstruct the fabrication of homogeneous coatings [1]. The interest was further boosted by the possibility to control such processes and to use them to manufacture functional layers on the nanometer scale [2,3]. The stability of ultrathin films is dominated by the effective molecular interactions between the substrate and the film surface [4]. They represent, for instance, long-range van der Waals forces which increase (decrease) the pressure in the film if they are attractive (repulsive) [5]. However, to determine the emerging length scale and pattern for unstable films a study of the film dynamics is required. Using a film thickness evolution equation obtained by long-wave approximation [6], the dewetting of a single layer of liquid is now reasonably well understood (see, e.g., Ref. [7]).

However, little is known about the behavior of two stacked ultrathin layers of simple or polymeric liquid on a solid substrate (see Fig. 1). Such a two-layer film allows for richer dynamics than a one-layer system, because both the free liquid-liquid and the free liquid-gas interface evolve in a coupled way. The evolution is driven by the effective molecular interactions between *all* the three interfaces separating the four material layers: substrate, liquid$_1$, liquid$_2$, and ambient gas. Although experimental studies investigated the different aspects of dewetting for two-layer films, like interface instabilities or the growth of holes [8–15], up to now no general theoretical description of the interface dynamics has been given [16]. The case of small interface deflections was investigated in Ref. [17] for a thickness of the lower layer, d_1, much larger than that of the upper one (d_2-d_1).

The most intricate questions for the first stage of dewetting of a two-layer system are *which* interface will become unstable, *where* does the film rupture, and *how long* will it take. This will determine the observability of the instability and the final morphology of the film. Experiments found a roughening of the liquid-liquid interface [12] or an instability of the liquid-gas interface [8,15]. Holes that evolve solely in the upper layer were also studied [9,10].

In this Rapid Communication, we derive and analyze coupled long-wave evolution equations for the two interfaces that are valid for all interface deflections and thickness ratios. We show that solely by changing the thickness ratio of the layers, one switches between different dominant instability modes. This leads to drastic changes of the pathway of dewetting from rupture at the substrate, to rupture at the liquid-liquid interface (see Fig. 2 below). Remarkably, for systems composed of two layers of very different thickness, i.e., with very different time scales for the rupture of the individual layers, the faster layer drives the evolution and accelerates the growth of surface modulations of the slower layer by orders of magnitude. We illustrate our results for two-layer systems of polystyrene (PS) and polymethylmetacrylate (PMMA), with silicon (Si) or silicon oxide (SiO) as substrates, like those studied experimentally in Refs. [9,11,15].

We believe our model can be used not only for the description of two-layer experiments with simple or polymeric liquids, but using an appropriate free-energy functional, also for a liquid film on a substrate with a stable but soft coating like a polymer brush [18] and, including driving terms, for studies of the transport of liquid droplets in liquid-liquid microfluidic systems [19].

Coupled film thickness equations. We obtain evolution equations for the film thicknesses h_1 and h_2 by simplifying the Navier-Stokes equations employing long-wave approximation [6]. Thereby a no-slip condition at the substrate, the continuity of the velocity field, and the balance of the stress tensors at the liquid-liquid and liquid-gas interfaces, are
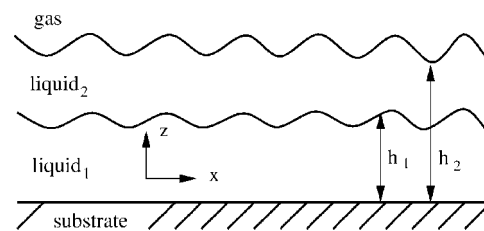

FIG. 1. Geometry of the two-layer system. The mean film thicknesses of the lower and upper layer are d_1 and d_2-d_1, respectively.
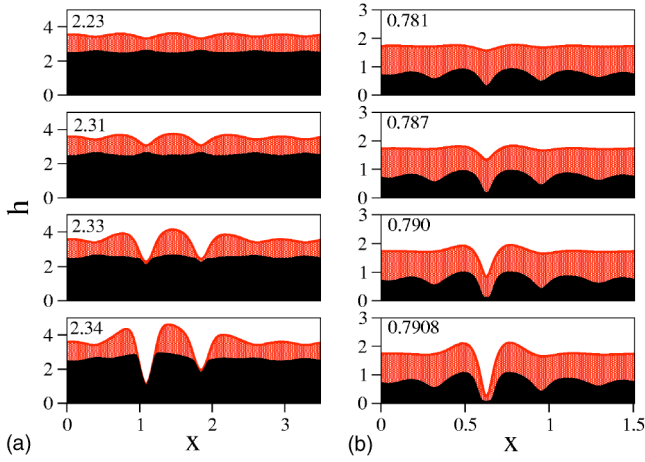
FIG. 2. Snapshots from time evolutions of a two-layer film for a Si-PMMA-PS-air system at dimensionless times (in units of τ_{up}) as shown in the insets. (a) At $d=1.4$ a varicose mode evolves, leading to rupture of the upper layer at the liquid-liquid interface. The ratio of the time scales derived from the upper and lower effective one-layer system is $\tau_{up}/\tau_{low}=0.066$. (b) At $d=2.4$ a zigzag mode evolves and rupture of the lower layer occurs at the substrate ($\tau_{up}/\tau_{low}=34.98$). The domain lengths are five times the corresponding fastest unstable wavelength and $\mu=\sigma=1$.

used. Considering an isothermal two-layer system, where both layer thicknesses are smaller than 100 nm, we neglect gravity and solely focus on the effective molecular interaction. For simplicity we only regard nonretarded long-range van der Waals forces resulting from dipole-dipole interactions between apolar materials. However, the inclusion of other forces, like, e.g., short-range polar forces [20] or slip boundary conditions [6] (that may be necessary for polymer films), is straightforward as for one-layer films. The details of the derivation will be presented elsewhere. We obtain [16]

$$\frac{\partial h_1}{\partial t} = \nabla \left(Q_{11} \nabla \frac{\delta F}{\delta h_1} + Q_{12} \nabla \frac{\delta F}{\delta h_2} \right),$$

$$\frac{\partial h_2}{\partial t} = \nabla \left(Q_{21} \nabla \frac{\delta F}{\delta h_1} + Q_{22} \nabla \frac{\delta F}{\delta h_2} \right), \qquad (1)$$

where $\delta F/\delta h_i$ with $i=1,2$ denotes functional derivatives of the total energy of the system,

$$F = \int [\rho_s + \rho_{VW}] d\mathbf{x}. \qquad (2)$$

It contains the densities of the surface energy $\rho_s = \frac{1}{2}[\sigma_1(\nabla h_1)^2 + \sigma_2(\nabla h_2)^2]$ and the energy for the van der Waals interaction $\rho_{VW} = -A_{g21s}/(12\pi h_2^2) - A_{21s}/(12\pi h_1^2) - A_{12g}/[12\pi(h_2-h_1)^2]$. The surface tensions σ_1 and σ_2 belong to the liquid-liquid and liquid-gas interface, respectively. A_{g21s}, A_{21s}, and A_{12g} are four- and three-index Hamaker constants, with subscripts s, 1, 2, and g referring to the substrate, liquid$_1$, liquid$_2$, and gas, respectively [21].

The symmetric matrix of the positive mobility factors Q_{ik} reads

$$Q = \frac{1}{3\mu_1} \begin{pmatrix} h_1^3 & \frac{3h_1^2}{2}\left(h_2 - \frac{h_1}{3}\right) \\ \frac{3h_1^2}{2}\left(h_2 - \frac{h_1}{3}\right) & \frac{(h_2-h_1)^3(\mu_1-\mu_2)}{\mu_2} + h_2^3 \end{pmatrix},$$

$$(3)$$

where μ_1 and μ_2 are the viscosities of liquid$_1$ and liquid$_2$, respectively. Note that for $d_2-d_1 \ll d_1$ and for small surface deflections Eqs. (1) simplify to those of Ref. [17]. Assuming two identical liquids, Eqs. (1) reduce to the well-known one-layer equation [6].

To compare with the well-understood one-layer systems, we nondimensionalize Eqs. (1) using scales derived from the upper layer as an effective one-layer system. We scale x with $\lambda_{up}=4\pi(d_2-d_1)^2\sqrt{\pi\sigma_2/|A_{12g}|}$, h_i with d_2-d_1, and t with $\tau_{up}=48\pi^2\mu_2\sigma_2(d_2-d_1)^5/A_{12g}^2$. The corresponding energy scale is $|A_{12g}|/16\pi^3(d_2-d_1)^2$. The ratios of the mean thicknesses, surface tensions, and viscosities are $d=d_2/d_1$, $\sigma=\sigma_2/\sigma_1$, and $\mu=\mu_2/\mu_1$, respectively. To compare with the lower layer as an effective one-layer system, one introduces in an analogous way the length scale λ_{low} and time scale τ_{low}.

We simulate the coupled time evolution of h_1 and h_2, Eqs. (1), in a one-dimensional domain using a semi-implicit time integration scheme and periodic boundary conditions. Initial conditions consist of flat layers with an imposed noise of amplitude 0.001. Alternative pathways of dewetting that occur for different thickness ratios d are presented in Fig. 2 using a Si-polymethylmethacrylate-polystyrene-air system (Si-PMMA-PS-air) as an example. Figure 2(a) shows that for a relatively small $d=1.4$ the two interfaces start to evolve deflections that are in antiphase, indicating the dominance of a varicose mode. When the liquid-gas interface approaches the liquid-liquid interface the latter starts to move downwards due to dynamical effects. This pathway leads to rupture of the upper layer, i.e., at the liquid-gas interface. On the contrary, Fig. 2(b) shows that for a larger $d=2.4$ the growing deflections of the two interfaces are in phase, indicating the dominance of a zigzag mode. As a consequence, here the lower layer ruptures, i.e., rupture occurs at the substrate.

Note that in both Figs. 2(a) and 2(b), at the moment of rupture, the respective nonruptured layer is also in an advanced stage of its evolution, leading to subsequent rupture. This is remarkable, because their time scales as effective one-layer systems are 15 [Fig. 2(a)] and 35 times [Fig. 2(b)] slower than the time scales for the respective fast layer. The ratio of the time scales τ_{up}/τ_{low} is proportional to $(d-1)^5$, i.e., for a lower layer ten times thicker than the upper one, the rupture time of the lower layer is about 5 orders of magnitude larger than the one of the upper layer. However, a simulation for a Si-PMMA-PS-air system with $d_1=10$ and $d_2-d_1=1$ shows that at rupture of the upper layer at $t=0.61\tau_{up}=3.99\times10^{-5}\tau_{low}$ the lower layer already evolved a depression of one-fourth of its thickness. If the lower layer is the fast one, the effect also exists, but is less pronounced.

In both cases, the acceleration of the rupture of the slower layer is caused by the direct coupling of the layers via the liquid-liquid interface. The fast evolution of the thinner layer deforms the interface and brings the thicker layer beyond the
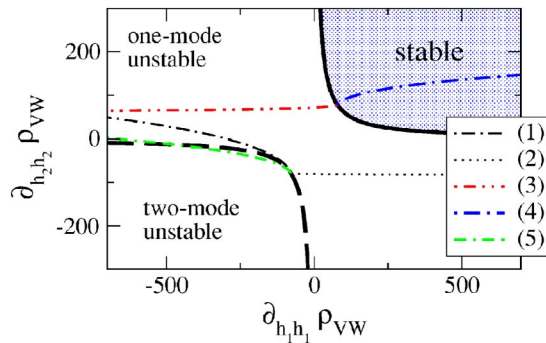
FIG. 3. Stability diagram for fixed scaled coupling $\partial_{h_1 h_2}\rho_{VW}$ $= 8\pi^2 A_{12g}/|A_{12g}|$. Shown are the stability threshold (solid line) and the boundary between unstable one- and two-mode regions (dashed line). The thin lines represent the trajectories for commonly studied systems: (1) Si-PMMA-PS-air, (2) SiO-PMMA-PS-air, (3) SiO-PS-PDMS-air, (4) Si-PS-PDMS-air, and (5) Si-PDMS-PS-air. The Hamaker constants were calculated as detailed below [21].

slow linear stage of its evolution. If the upper layer is the driving layer the process is, in addition, dynamically enforced because the liquid-liquid interface is "pushed away" by the advancing liquid-gas interface.

Linear stability analysis. A deeper understanding of the different pathways can be reached by studying the linear stability of the initial flat layers. We linearize Eqs. (1) for small disturbances $\chi_i \exp(\beta t)\cos(kx)$ for $i=1,2$, where k, β, and $\boldsymbol{\chi}=(\chi_1,\chi_2)$ are the wave number, growth rate, and amplitudes of the disturbance, respectively. The dispersion relation $\beta(k)$ is obtained solving the resulting eigenvalue problem $[k^2\boldsymbol{Q}\cdot\boldsymbol{E}(k)+\beta\boldsymbol{I}]\boldsymbol{\chi}=\boldsymbol{0}$, where $\boldsymbol{Q}$ is the scaled mobility matrix and $\boldsymbol{E}$ is derived from the free-energy Eq. (2) as $E_{ij} = \partial_{h_i h_j}\rho_{VW}+\delta_{ij}\tilde{\sigma}_i k^2$ ($\tilde{\sigma}_1=1$, $\tilde{\sigma}_2=\sigma$, and $\delta_{ij}=1$ for $i=j$ and zero otherwise). The stability threshold shown as a solid line in Fig. 3 is determined by $\boldsymbol{E}$ for disturbances of infinite wavelength, i.e., $k=0$. The system is linearly stable for

$$\det \boldsymbol{E} > 0 \text{ and } E_{11} > 0 \text{ at } k=0. \qquad (4)$$

An instability sets in if at least one of the conditions (4) is violated. This implies that the two-layer film can be unstable even if both, $\partial_{h_1 h_1}\rho_{VW}$ and $\partial_{h_2 h_2}\rho_{VW}$ are positive, i.e., if the effective one-layer systems related to these terms are both stable.

Fixing the Hamaker constants, i.e., the combination of materials, and changing d, one finds a line (trajectory) in the stability diagram (Fig. 3) as shown for a variety of experimentally studied systems. Interestingly, for van der Waals interactions calculated as detailed in [21], one can show that such a trajectory *cannot* cross the stability threshold, i.e., it is not possible to stabilize such a two-layer system by solely changing d. For instance, for the Si-PMMA-PS-air system the second condition in (4) is violated for all d and the system is always unstable. At $d=1$, i.e., for a vanishing upper layer, the system is on the boundary between the one- and the two-mode regions (dashed line). For $1<d<2.3$ the unstable mode is an asymmetric varicose mode. A corresponding dispersion relation $\beta(k)$ is shown for $d=1.4$ in Fig. 4
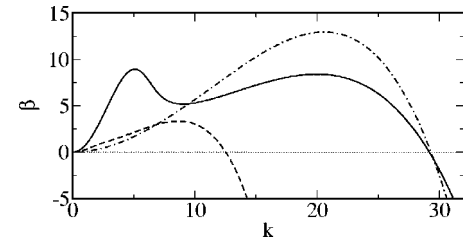

FIG. 4. Dispersion relations $\beta(k)$ for a Si-PMMA-PS-air system at $d=1.4$ (dashed line, varicose mode) and $d=2.4$ (dot-dashed line, zigzag mode) for parameters as in Fig. 2; and $4\beta(k)$ for a SiO-PMMA-PS-air system at $d=2.16$ (solid line) for $\mu=1$ and $\sigma=10$.

[compare to the time evolution in Fig. 2(a)]. For $d>2.3$, i.e., for smaller thicknesses of the lower layer, the unstable mode is an asymmetric zigzag mode. Figure 4 gives $\beta(k)$ for $d=2.4$ corresponding to the time evolution shown in Fig. 2(b). For the fastest mode the zigzag mode is strongly asymmetric, i.e., the deflection of the liquid-liquid interface dominates the linear stage of the evolution. Note that $\beta(k)$ and the dominant mode type depend on σ and μ, whereas the stability *does not*.

Further on, the simultaneous action of the van der Waals forces between the three interfaces allows for dispersion relations with two maxima. An experimental system showing this unusual form of $\beta(k)$ can be realized with a substrate that is less polarizable than both layers. This is the case for the SiO-PMMA-PS-air system [21]. A dispersion relation showing maxima of equal height is given for $d=2.16$ and $\sigma=10$ in Fig. 4. The maxima at small and large k correspond to strongly asymmetric zigzag and varicose modes, respectively. This implies that the larger (smaller) wavelength will predominantly be seen at the liquid-gas (liquid-liquid) interface [Fig. 5(a)]. Increasing (decreasing) the ratio of the surface tensions strengthens the smaller (larger) wavelength.
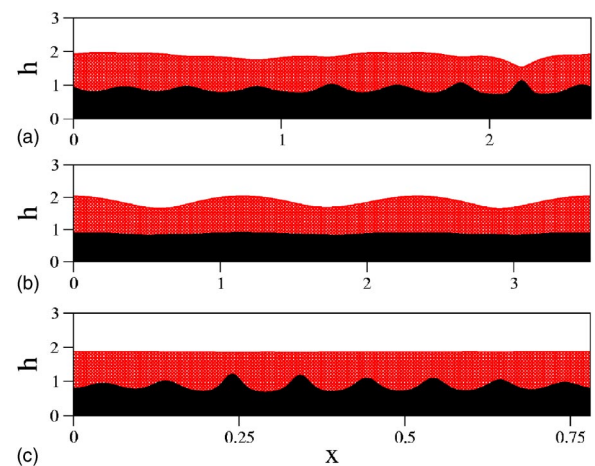

FIG. 5. Single snapshots from time evolutions of a SiO-PMMA-PS-air system for $d=2.16$, $\mu=1$, and different σ. (a) The respective evolutions of the two interfaces are dominated by modes of different wavelengths ($\sigma=10$, $t=3.83$). In (b) and (c) the evolution is dominated by the liquid-gas and the liquid-liquid interface, respectively ($\sigma=5$, $t=3.9$ and $\sigma=100$, $t=0.52$).

This implies that solely changing σ by adding an otherwise passive surfactant, one can switch from an evolution entirely dominated by the liquid-liquid interface to one dominated by the liquid-gas interface. This illustrates Fig. 5 by single snapshots from the nonlinear time evolutions for different σ.

To conclude, we have derived coupled evolution equations for a thin liquid two-layer film driven by long-range van der Waals forces. The system represents the most general form of coupled evolution equations for two conserved order-parameter fields in a relaxational situation and is apt to describe a broad variety of experimentally studied two-layer systems [25]. Linear and nonlinear analysis have shown that the mobilities have no influence on the stability threshold, but determine the length and time scales of the dynamics. We have shown that for a two-layer system *both* interface deflection modes—zigzag and varicose—may be unstable and lead to rupture at the substrate or the liquid-liquid interface. Remarkably, the faster layer accelerates the evolution of the slower layer even if the latter is rather thick, implying that its rupture time may be shortened by orders of magnitude.

[1] G. Reiter, Phys. Rev. Lett. **68**, 75 (1992).

[2] M. Mertig *et al.*, Appl. Phys. A: Mater. Sci. Process. **66**, S565 (1998).

[3] U. Thiele, M. Mertig, and W. Pompe, Phys. Rev. Lett. **80**, 2869 (1998).

[4] E. Ruckenstein and R. Jain, J. Chem. Soc., Faraday Trans. 2 **70**, 132 (1974).

[5] J. N. Israelachvili, *Intermolecular and Surface Forces* (Academic, London, 1992).

[6] A. Oron, S. H. Davis, and S. G. Bankoff, Rev. Mod. Phys. **69**, 931 (1997).

[7] U. Thiele, Eur. Phys. J. E **12**, 409 (2003), and other contributions of the Focus Point in Eur. Phys. J. E 12.

[8] A. Faldi, R. J. Composto, and K. I. Winey, Langmuir **11**, 4855 (1995).

[9] P. Lambooy, K. C. Phelan, O. Haugg, and G. Krausch, Phys. Rev. Lett. **76**, 1110 (1996).

[10] Q. Pan, K. I. Winey, H. H. Hu, and R. J. Composto, Langmuir **13**, 1758 (1997).

[11] M. Sferrazza *et al.*, Phys. Rev. Lett. **78**, 3693 (1997).

[12] M. Sferrazza *et al.*, Phys. Rev. Lett. **81**, 5173 (1998).

[13] M. O. David, G. Reiter, T. Sitthai, and J. Schultz, Langmuir **14**, 5667 (1998).

[14] C. Renger, P. Müller-Buschbaum, M. Stamm, and G. Hinrichsen, Macromolecules **33**, 8388 (2000).

[15] M. D. Morariu, E. Schäffer, and U. Steiner, Eur. Phys. J. E **12**, 375 (2003).

[16] As pointed out to us by A. Sharma, a predecessor of Eqs. (1), in terms of pressures rather than energy variations, is given in Ref. [22]. The system given in Ref. [23] can be transformed into the one in Ref. [22] when neglecting surface viscosity.

[17] F. Brochard-Wyart, P. Martin, and C. Redon, Langmuir **9**, 3682 (1993).

[18] G. Reiter, J. Schultz, P. Auroy, and L. Auvray, Europhys. Lett. **33**, 29 (1996).

[19] O. D. Velev, B. G. Prevo, and K. H. Bhatt, Science **426**, 515 (2003).

[20] A. Sharma, Langmuir **9**, 861 (1993).

[21] The four-index Hamaker constants are calculated using an equivalent of Eq. (11.13) of Ref. [5] that is based on the assumption that the main absorption frequencies of all involved media are about $\nu = 3 \times 10^{15}$ Hz and that the zero frequency contribution is neglectable. This yields

$$A_{ijkl} \approx \frac{3h\nu_e}{8\sqrt{2}} \frac{(n_i^2 - n_j^2)(n_l^2 - n_k^2)}{(n_i^2 + n_j^2)^{1/2}(n_l^2 + n_k^2)^{1/2}[(n_i^2 + n_j^2)^{1/2} + (n_l^2 + n_k^2)^{1/2}]}.$$

The three-index Hamaker constants are obtained by $A_{ijk} = A_{ijjk}$. For the Si/PMMA/PS/air system one obtains $A_{12g} = 1.49 \times 10^{-20}$ J, $A_{21s} = 3.81 \times 10^{-20}$ J, and $A_{g21s} = -23.02 \times 10^{-20}$ J, whereas the SiO/PMMA/PS/air system is characterized by $A_{12g} = 1.49 \times 10^{-20}$ J, $A_{21s} = 0.02 \times 10^{-20}$ J and $A_{g21s} = 0.15 \times 10^{-20}$ J. The used refractive indices of the media are $n_{PS} = 1.59$, $n_{PDMS} = 1.43$, $n_{PMMA} = 1.49$, $n_{Si} = 4.11$, and $n_{SiO} = 1.48$ [15]. We generally neglect acoustic contributions to the disjoining pressure [24], because the acoustic modes are not confined to the individual liquid layers [15].

[22] D. Bandyopadhyay, Masters thesis, Ind. Inst. Tech. Kanpur, 2001.

[23] K. D. Danov *et al.*, Chem. Eng. Sci. **53**, 2809 (1998).

[24] E. Schäffer and U. Steiner, Eur. Phys. J. E **8**, 347 (2002).

[25] For coupled evolution equations for one conserved and one nonconserved order parameter describing self-propelled chemically driven droplets, see U. Thiele, K. John, and M. Bär, Phys. Rev. Lett. **93**, 027802 (2004).